Consultancy Report

Cadent Gas Ltd: Alrewas EM Offtake

Determination of Impact of Two Orifice Plates Reverse Installation on Flow Measurement by CFD Study

End Customer: Cadent Gas Ltd

End Customer Reference Number: 3200905035

i-Vigilant Reference Number: iVJob22008-RPT-001-I02

Document File Name: MSS-PM-3307572-C-RPT-01 Rev 01 i-Vigilant CFD Study on Orifice Plates Reverse Installation.docx

Document Status: Final

Authorizations:

	Name	Function	Signature
Developed by:	Nadezhda A. Pashnina	Measurement Consultant	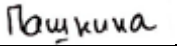
Reviewed by:	Brian Law	Measurement Consultant	
Released by:	Nadezhda A. Pashnina	Measurement Consultant	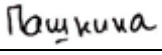

Revision History

Rev	Status	Description	Date	Report By	Reviewed By
00	Preliminary	Issued for internal review	13/04/2022	N. Pashnina	B. Law
01	Final	Issued to the client	14/04/2022	N. Pashnina	B. Law

Emerson Automation Solutions
Measurement Consultancy Group
Aberdeen Solutions Centre, 1 Harvest Avenue, D2 Business Park, Dyce,
Aberdeen, AB21 0BQ
www.Emerson.com

Table of Contents

List of Figures

List of Tables

1 EXECUTIVE SUMMARY

This report provides the results of the Computational Fluid Dynamics (CFD) study of the dry gas flow through a standard single stream 18'' orifice plate flow meter installed in the Alrewas EM NTS Offtake to LDZ described in section 5.

The study aimed to determine the impact on the flow measurement caused by two orifice plates 295/5 and ALRE5036 that had been installed in the reverse orientation at Alrewas EM NTS Offtake in the period from 23/05/2019 to 23/02/2021.

The CFD study of both orifice plates has been undertaken to determine the correction in the discharge coefficient considering three flow rates forming six test cases outlined in section 2.4 for both forward and reverse orientation of the orifice plates.

The modelling approach is covered in section 6, where the computational domain is set by the orifice plates and pipework geometry, the mesh grid and boundary conditions are specified for the selected RANS-based turbulence model k-ω SST. ANSYS CFX and ANSYS Fluent solvers are considered for the study. The CFD computational results obtained using the selected model settings were compared in Appendix 3 with the results available in the publication [11].

The CFD modelling results for the orifice plates 295/5 and ALRE5036 are presented in section 7, where the effect of reverse installation on fluid velocity, static pressure along the wall, pressure loss, mass flow rate and the discharge coefficient is shown.

The quality of the model has been assessed by comparison of the discharge coefficient calculated using the standard ISO 5167-2:2003 and obtained as the results of CFD modelling for the forward orientation of both orifice plates. The error between two coefficients have been found within 0.5 % what is within the uncertainty of 0.7 % set in the standard [6] for $0.6<\beta\leq0.75$.

In the reverse orientation the value of the pressure drop across the orifice plates has been found lower than in the forward orientation of the orifice plates. Therefore, the recorded mass flow rate in the period of interest should be increased by the following proposed corrections calculated as an average of the results obtained independently in two CFD solvers as the difference in correction obtained for the same orifice plate is within the discharge coefficient uncertainty of 0.7 %:

- The correction for the orifice plate 295/5 is around 5.6 % based on CFX solver, and 4.9 % based on Fluent solver. The average correction for all modelled flow rates is calculated as **5.27 %**.
- The correction for the orifice plate ALRE5036 is around 4.1 % based on CFX solver, and 3.6 % based on Fluent solver. The average correction for all modelled flow rates is calculated as **3.85 %**.

The sensitivity of the calculated correction to the variation of the modelled flow rates has been found insignificant and may be neglected. The sensitivity of the corrections to the geometry of the orifice plates demonstrated in section 7.3 suggests that the corrections may change with variation of the orifice plate parameters away from the values suggested for CFD.

The significant difference in the proposed corrections of the discharge coefficient for two orifice plates 295/5 and ALRE5036 has been explained by the difference in the angle of bevel of 0.5º, and the difference in the orifice plate thickness 'e' of 7.015 mm and 7.45 mm respectively.

2 INTRODUCTION

2.1 Purpose

The purpose of this report is to determine the impact on the flow measurement caused by two orifice plates 295/5 and ALRE5036 that had been installed in the reverse orientation at Alrewas EM NTS Offtake. The determination should be carried out by utilising a high-performance computational fluid dynamics software tool.

2.2 Background

Alrewas EM NTS Offtake supplies gas to the East Midlands LDZ. The metering system comprises of a standard single stream 18'' orifice plate with a maximum station flowrate of 16 million Sm3/d as detailed in the executive summary of the meter error [1].

On 23/02/2021 the plate was removed for inspection and was found to have been installed in the incorrect orientation (bevelled edge facing upstream).

Subsequent investigation found that on 20/05/2020 the orifice plate was changed as part of an ME/2 annual validation. A review of the photographs showed that the plate that was removed on this date was also in the incorrect orientation. A review of the photographs from the previous ME/2 annual validation on 23/05/2019 showed that the plate prior to this date was correctly installed. Therefore, the period in which the meter was in error was between 23/05/2019 and 23/02/2021.

Initial studies undertaken by Cadent metering technical consultants indicated a high likelihood the error would be in excess of the 50 GWh Significant Measurement Error threshold. As the standards do not contain a sufficient information to assess the impact imposed by the reverse orientation of the orifice plates, alternative methods of evaluating the magnitude of the correction are required.

i-Vigilant Technologies Limited contracted Emerson to carry out a computational fluid dynamics (CFD) study on the Alrewas EM NTS Offtake to identify the impact on the flow measurement caused by the reverse orientation of two orifice plates 295/5 and ALRE5036 and issue a single report predicting an expected shift in the discharge coefficient of both orifice plates.

2.3 Methods of Investigation

The numerical simulation tool and the CFD simulation methods have been proposed to investigate the impact of the reverse orientation of the orifice plate on the flow measurement by assessing the shift in the discharge coefficient of the orifice plates.

To evaluate the shift in the discharge coefficient a series of simulations have been carried out for both the forward and reverse orientations of the orifice plates, so that the results of the two directions can be compared.

CFD provides well-established tools for the prediction of the flow parameters. For the present study the flow has been assumed steady, turbulent and compressible throughout the computational domain and the Reynolds-Averaged Navier-Stokes (RANS) model, the RANS-based turbulence k-ω SST model [8] were used for numerical simulation. ANSYS CFX and ANSYS Fluent solvers are considered for the study.

2.4 Scope

Emerson will provide a CFD study to determine the impact on the flow measurement caused by two orifice plates 295/5 and ALRE5036 installed in reverse orientation. The test cases were agreed with Cadent Gas Ltd by i-Vigilant Technologies Limited and detailed in Table 1. Other parameters can be found in section 5.

Table 1: Test Cases

Parameter	Case 1 Lo Flow	Case 2 Typical Flow	Case 3 Hi Flow	Case 4 Lo Flow	Case 5 Typical Flow	Case 6 Hi Flow
Orifice Plate	295/5	295/5	295/5	ALRE5036	ALRE5036	ALRE5036
Orifice Plate Diameter at Process Conditions, mm	309.9425	309.9425	309.9425	309.94476	309.94476	309.94476
Orifice Plate Thickness ‘E’, mm	9.2370	9.2370	9.2370	9.2873	9.2873	9.2873
Orifice Plate Thickness ‘e’, mm	7.015	7.015	7.015	7.450	7.450	7.450
Orifice Plate Angle of Bevel, º	44.5	44.5	44.5	44.0	44.0	44.0
Orifice Plate Orientation	Forward & Reverse	Forward & Reverse	Forward & Reverse	Forward & Reverse	Forward & Reverse	Forward & Reverse
Mass Flowrate, kg/h	86,519.10	131,659.50	176,799.90	86,519.10	131,659.50	176,799.90
Velocity*, m/s	3.2530	4.9502	6.6474	3.2530	4.9502	6.6474
Reynolds Number	5.88E+06	8.95E+06	12.01E+06	5.88E+06	8.95E+06	12.01E+06
Pipe Diameter at Process Conditions, mm	432.3053					
Process Pressure, barg	56					
Process Temperature, ºC	8.5					
Molecular Weight**, kg/kmol	17.7472					
Process Compressibility Factor**, dimensionless	0.85843					
Process Density**, kg/m^3	50.3333					
Dynamic Viscosity**, cP	0.01204					

* the velocity is calculated for the mass flow rate and the pipeline diameter.

** the values are calculated based on the gas composition provided in the document [7].

In addition to the agreed test cases provided in Table 1, several additional tests have been computed to assess the effect of the plate dimensions (thickness ‘e’ and angle of bevel) on the shift in discharge coefficient and explain the difference in the calculated corrections for the orifice plates 295/5 and ALRE5036.

Additionally, the tests required for comparison with the CFD computation results available in the publication [11] have been performed using the model setup proposed in the present report (refer to Appendix 3).

3 ABBREVIATIONS AND DEFINITIONS

Abbreviations and definitions used within this document presented in Table 2.

Table 2: List of Abbreviations and Definitions

Abbreviation	Definition
2D	Two-dimensional
3D	Three-dimensional
ANSYS CFX/Fluent	High-performance computational fluid dynamics software tool
BS	British Standard
CAD	Computer Aided Design
CFD	Computational Fluid Dynamics
EM	East Midlands
ISO	International Organization for Standardization
LDZ	Local Distribution Zone
NTS	National Transmission System
RANS	Reynolds-Averaged Navier-Stokes
SST	Shear Stress Transport

4 NOMENCLATURE

The units of measurement used within the document are detailed in Table 3. The used units and symbols defined in the standard BS 350 [5].

Table 3: Units of Measurement

Symbol	Description	Special Name
bar	pressure	bar
d	time	day
ft	length	feet
g/mol	molar mass	gram per mole
h	time	hour
in	length	inch
K	thermodynamic temperature	kelvin
kg	mass	kilogram
kg/h	mass flow rate	kilogram per hour
kg/m^3	density	kilogram per cubic metre
kg/s	mass flow rate	kilogram per second
m	length	metre
m/s	velocity	metre per second
mol	amount of substance	mole
P	dynamic viscosity	poise
s	time	second
º	plane angle	degree of angle
ºC	Celsius temperature	degree Celsius

It is a common practice to differentiate between:

- gauge and absolute pressures by adding the further letters ‘g’ and ‘a’ to make ‘barg’ and ‘bara’ respectively.
- standard and normal reference conditions for volume flow rate by adding the fore-letters ‘S’ and ‘N’ to make ‘Sm^3/h’ and ‘Nm^3/h’ respectively.

The prefixes used within the document are detailed in Table 4.

Table 4: Decimal Multiples and Submultiples Prefixes

Symbol	Description	Special Name
k	10^3	kilo
c	10^{-2}	centi
m	10^{-3}	milli

5 INSTALLATION DESCRIPTION

5.1 Alrewas EM NTS Offtake Design

The Alrewas EM NTS offtake meter stream layout equipped with the orifice plate flow meter is shown on Figure 1 and Figure 2.

A flow element (orifice plate) is installed into a pipeline in which natural gas is running full. The presence of the orifice plate causes a static pressure difference between the upstream and downstream sides of the plate. The measured pressure drop allows calculation of the mass flow rate using the ISO 5167-2:2003 equations [6].

Figure 1: Meter Stream Layout

Figure 2: Satellite View of Meter Stream Layout

The details of the orifice fitting, meter stream, orifice plates and process conditions have been obtained from the document [7] provided to confirm the basis for CFD simulation. The details are provided in the following sections.

5.2 Orifice Fitting and Meter Stream

The following tables contain the extracts from the document [7] and contain the basis for the CFD analysis.

Table 5: Metrology of Orifice Fitting

Parameter	7702835/1
Measurement Temperature (assumed), ºC	20
Measured Upstream Diameter, in (m)	17.022 (0.43236)
Temperature Expansion Factor (assumed), 1/ºC	0.000011
Upstream Straight Length, ft and in (m)	33’ 0 1/8” (10.06158)
Downstream Straight Length, ft and in (m)	10’ 5 7/8” (3.19723)
Tappings (assumed)	Flange
Distance of Tappings from Orifice Plate, mm	25.4
Tapping Diameter (assumed), mm	6

Table 6: Metrology of Meter Stream

Parameter	Alrewas EM
Upstream Straight Length*	49 D
Downstream Straight Length	22.5 D
Flow Conditioning*	Possibly at 23D
Upstream Pipework*	45 Degree Bend and Valve

* not considered in modelling

5.3 Orifice Plates

The orifice plates geometry taken from the calibration certificates is provided in Table 7.

Table 7: Metrology of Orifice Plates

Parameter	295/5	ALRE5036
Calibration Certificate	DNV-GL: 14474	DNV-GL: 14634-1
Certificate Issue Date	8th May 2019	5th August 2019
Laboratory Temperature, ºC	19.5	20.0
Bore Diameter measured at Laboratory Temperature, mm	309.9971	310.0018
Plate Thickness ‘E’, mm	9.2370	9.2873
Thickness ‘e’, mm	7.015	7.450
Angle of Bevel, degree of angle	44.50	44.00
Temperature Expansion Factor (assumed), 1/ºC	0.000016	0.000016

5.4 CFD Modelling Conditions

The orifice plates geometry corrected to the typical flowing conditions is provided in Table 8.

Table 8: Geometry and Process Conditions for CFD Modelling

Parameter	295/5	ALRE5036
Orifice Plate Bore Diameter 'd' corrected to Typical Flowing Temperature of 8.5 ºC, mm	309.9425	309.94476
Orifice Plate Thickness 'E', mm	9.2370	9.2873
Orifice Plate Thickness 'e', mm	7.015	7.450
b=E-e	2.222	1.8373
b/d	0.007	0.006
Angle of Bevel, º	44.50	44.00
Beta Ratio	0.71695	0.71696
Distance between Pressure Tappings, mm	60.0370	60.0873
Upstream Diameter 'D' corrected to Typical Flowing Temperature of 8.5 ºC, mm	432.3053	
Inlet Cross-sectional Area, mm^2	146781.39	
Typical Flowing Pressure, barg	56	
Typical Flow, Sm^3/h; kg/h; kg/s	175,000; 131,659.50; 36.5720833	
Typical Velocity, m/s	4.9502	
Typical Reynolds Number	8.95E+06	
Lo Flow, Sm^3/h; kg/h; kg/s	115,000; 86,519.10; 24.0330833	
Lo Velocity, m/s	3.2530	
Lo Reynolds Number	5.88E+06	
Hi Flow, Sm^3/h; kg/h; kg/s	235,000; 176,799.90; 49.1110833	
Hi Velocity, m/s	6.6474	
Hi Reynolds Number	12.01E+06	
Gas Molecular Weight*, kg/kmol	17.7472	
Process Compressibility Factor*, dimensionless	0.85843	
Product of Molecular Weight and Compressibility Factor***, kg/kmol	20.674021	
Process Density* at 8.5 ºC and 56 barg, kg/m^3	50.3333	
Dynamic Viscosity** at 8.5 ºC and 56 barg, cP	0.01204	

* calculated from composition provided in the document [7] using AGA8:1994 (neo-Pentane is added to nPentane)

** calculated from composition provided in the document [7] using API Natural Gas Viscosity F094 FloCALC.net v.1.8.2

*** used as an input to the models

The 2D CAD models of the Alrewas EM NTS offtake meter stream with orifice plates 295/5 and ALRE5036 at process conditions are shown on Figure 3 and Figure 4 respectively.

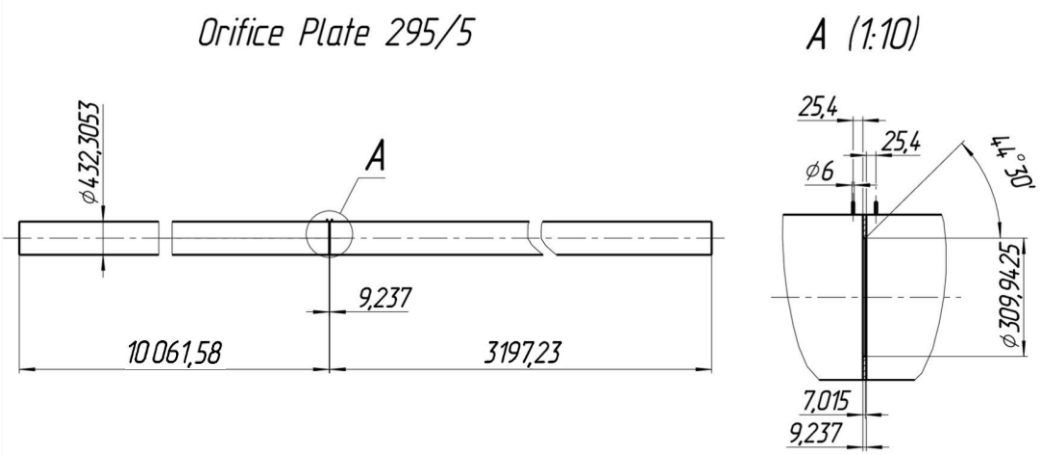

Figure 3: 2D Geometry of Meter Stream with 295/5 Orifice Plate

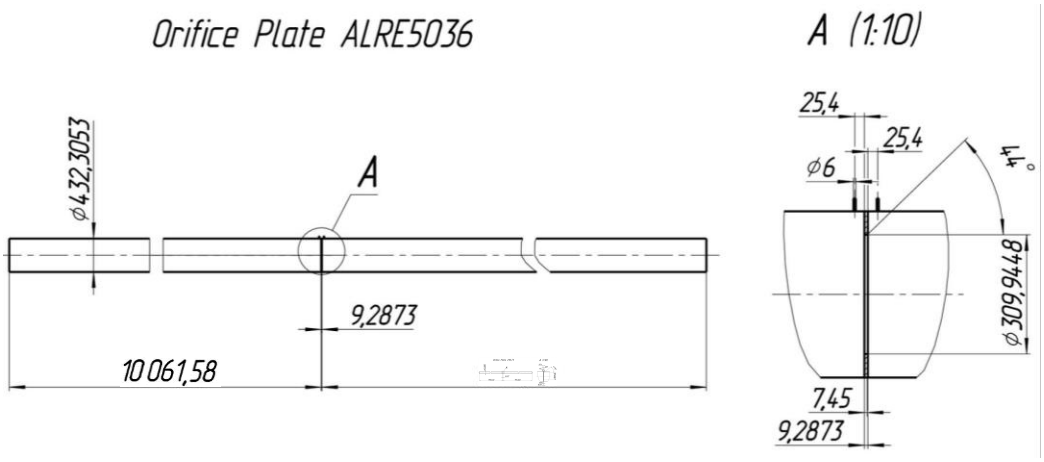

Figure 4: 2D Geometry of Meter Stream with ALRE5036 Orifice Plate

6 CFD MODELLING

CFD modelling involves four steps: (1) creating the model geometry and (2) mesh, (3) defining the physical models by model setup, and (4) defining the boundary and operating conditions.

ANSYS CFX and ANSYS Fluent solvers are considered for the modelling.

6.1 Geometry

Cadent Gas Ltd supplied the pipework information of the Alrewas EM NTS Offtake shown on Figure 1 and Figure 2. Based on the provided information the model suitable for CFD study was created. The following pipework elements are not considered in the model: thermowell, upstream valve, and upstream 45-degree bend.

Figure 5 illustrates the computational domain. The upstream length of 23D is selected for the modelling and defined by the position of the flow conditioner possibly installed upstream to the orifice plate.

For the modelling of the forward orientation of the orifice plate the flow from left to right is considered, and for the reverse orientation the flow direction is swapped to from right to left. Therefore, the downstream length is set to 23D as well, and the overall length of the computational domain in the pipe axial direction forms 46D plus the orifice plate thickness ‘E’.

The flow through the orifice plate is assumed steady and axisymmetric to reduce the number of mesh elements and consequently computational time. Therefore, the model is limited by the axis of rotational symmetry along the pipe. The 3D model is obtained by rotation of the 2D geometry by the rotation angle (3º for CFX and 7.5º for Fluent) as shown on Figure 6.

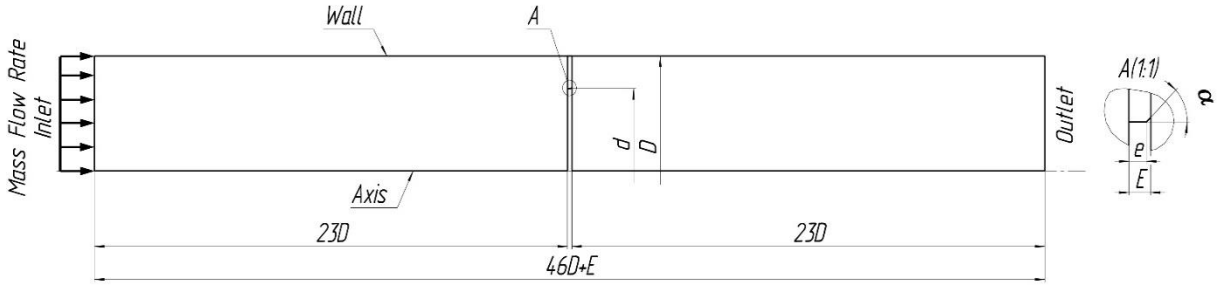

Figure 5: 2D Model Geometry

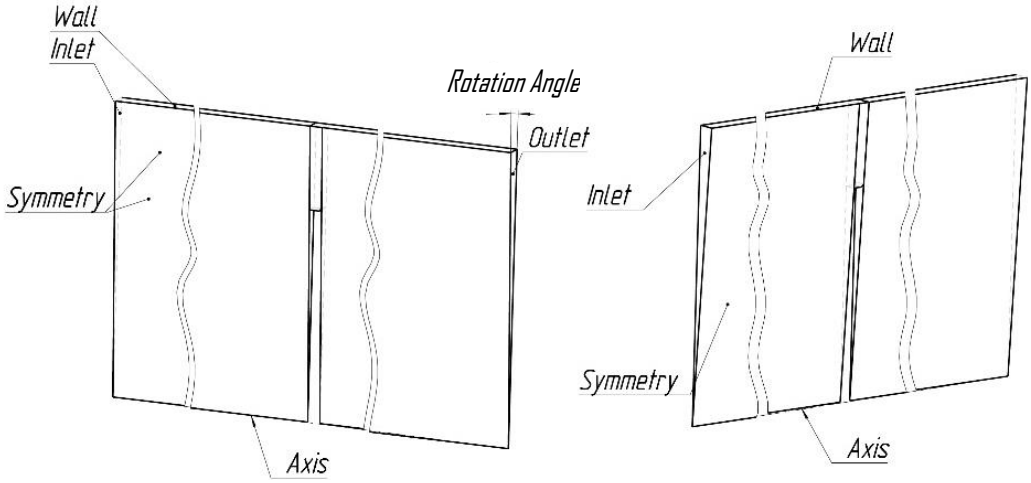

Figure 6: 3D Model Geometry

6.2 Mesh Grid

The partial differential equations describing the fluid flow are non-linear and shall be solved numerically. To do so, the 3D model geometry is split into small elements (finite volumes) and the equations are solved inside each of these. The collection of all elements is called a mesh.

The non-structured hexahedral mesh [4] used for CFD simulation is shown in Figure 7 around the orifice plate edge. The mesh consists of nearly 994,000 nodes and 500,000 elements positioned in one layer.

The wall-adjacent elements form the prism layer, and the element size is set using the non-dimensional wall distance parameter $y^+<100$.

The region upstream and downstream of the plate is filled with square elements; this ensured that the element structure surrounding the plate is the same for both the forward and reverse orientations. The size of these square elements is 0.1 mm, giving 22 elements along the orifice-edge and 70 along the bevel. Outside the orifice plate region, the grid was expanded to the inlet and outlet planes to optimise the count of the elements.

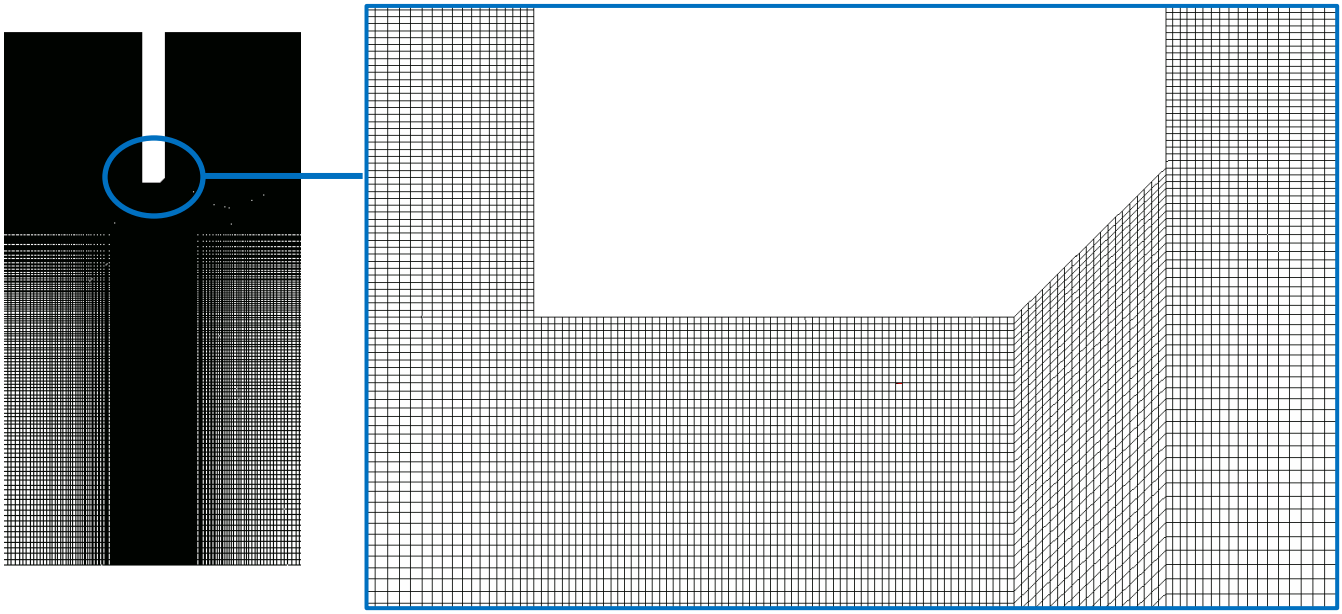

Figure 7: Mesh Grid

6.3 Model Setup

To perform the numerical simulation, the Reynolds-Averaged Navier-Stokes equations (RANS) are chosen as a mathematical model. The RANS-based turbulence model k-ω SST [8] is selected for both ANSYS CFX and ANSYS Fluent solvers.

The k-ω SST turbulence model is suitable for modelling of complex turbulent flows. It is adaptive to the wide range of the y^+ distance parameter (from 0 to 100) and accurately predicts the point of flow separation and the area of separation bubble at adverse pressure gradients. The k-ε models are not as good as k-ω models at y^+ values close to zero what is specific for zero velocity condition on the walls.

The k-ω SST turbulence model is a two-equation eddy-viscosity model. The shear stress transport (SST) formulation combines the best of two worlds. The use of a k-ω formulation in the inner parts of the boundary layer makes the model directly usable all the way down to the wall through the viscous sub-layer. The SST formulation also switches to a k-ε behaviour in the free-stream and thereby avoids the common k-ω problem that the model is too sensitive to the inlet free-stream turbulence properties.

The discretization methods used in the model are second order for the momentum and mass equations, and first for the turbulence equations. The convergence of the solution for scaled residuals is set at 10^{-5}. The settings of ANSYS CFX and Fluent are provided in Appendix 2.

6.4 Boundary and Operating Conditions

The RANS equations with standard no-slip boundary conditions on the smooth walls and a zero-gradient boundary condition at the outlet are established.

The boundary and operating conditions are defined by the test cases detailed in Table 1 in section 2.4 and set in solvers as shown in in Appendix 2. The mass flow rate is set as a boundary condition at the inlet along with the evenly distributed velocity profile.

7 RESULTS

This section presents the CFD modelling results for the Alrewas EM NTS offtake flow meter with the orifice plates 295/5 and ALRE5036 at the conditions defined by the selected test cases (refer to section 2.4).

The modelling results have been obtained using ANSYS CFX and ANSYS Fluent solvers and both results are considered for calculation of the correction imposed by reverse installation of the orifice plates.

7.1 Velocity

This section provides the CFD computation results obtained for velocity upstream and downstream of the Alrewas EM NTS offtake flow meter with the orifice plates 295/5 and ALRE5036 at the flow rate of 131,659.50 kg/h.

Figure 8 and Figure 9 show the velocity field and flow lines.

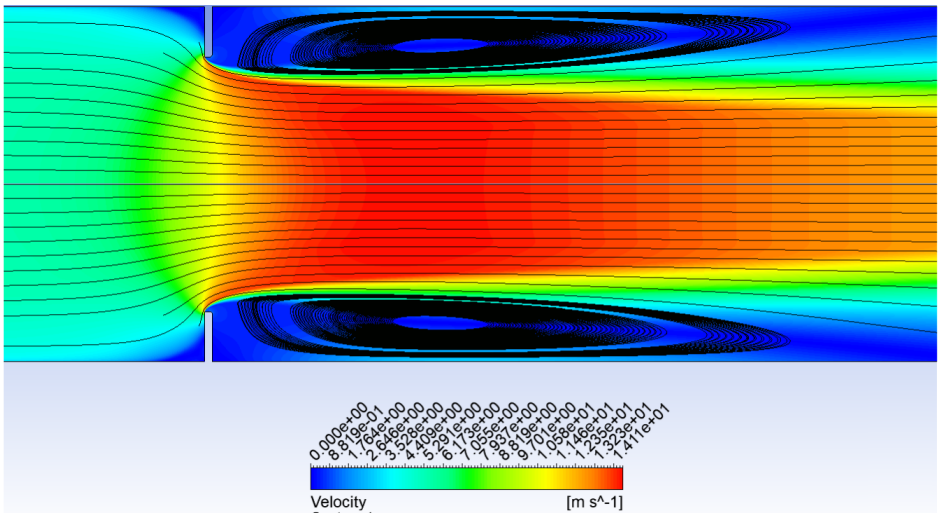

Figure 8: Velocity Field and Flow Lines for Forward Orientation of Orifice Plates

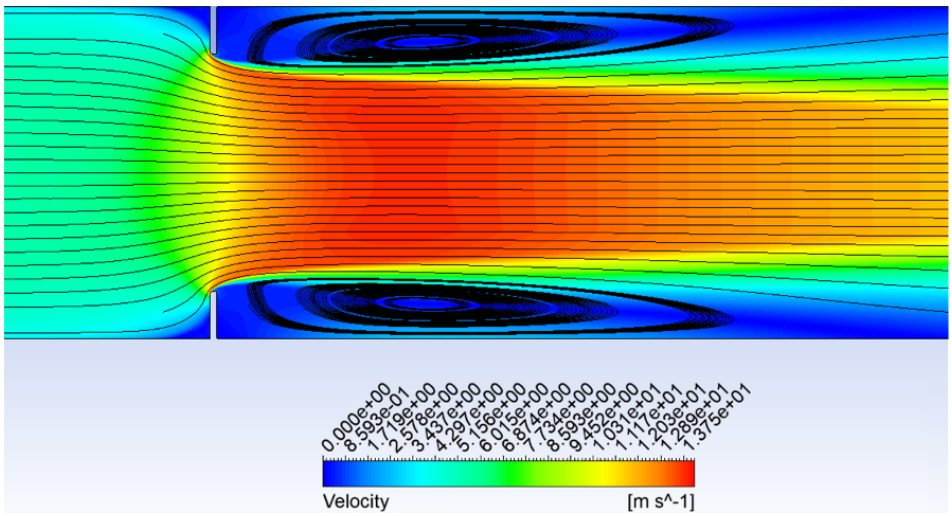

Figure 9: Velocity Field and Flow Lines for Reverse Orientation of Orifice Plates

Figure 10 and Figure 11 show the velocity profile along the wall for the orifice plates 295/5 and ALRE5036 respectively at 6D, 8D and 10D locations both upstream and downstream as well as at both pressure tappings P1 and P2. Theoretical velocity profile for smooth wall ('Theory in the graphs legend') is defined by the logarithmic law [9].

Upstream of the orifice plate the velocity profile is very close to the logarithmic law. Downstream of the orifice plate the velocity profile completely recovered at 10D and matches the logarithmic law for both forward and reverse orientations.

For forward orientation the velocities are higher at P1 and P2, but lower at downstream 6D, 8D and 10D locations.

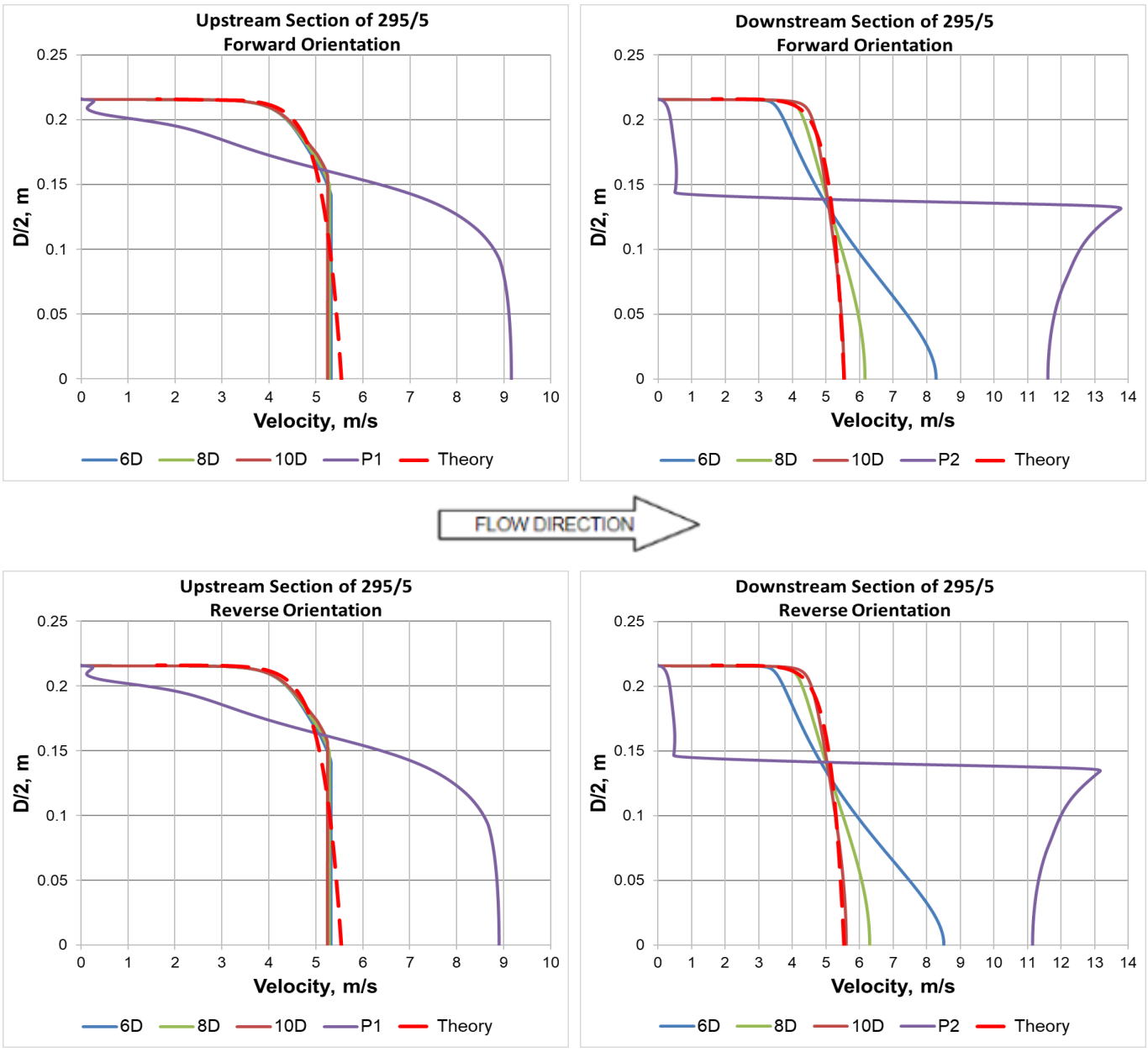

Figure 10: Velocity Profiles Upstream and Downstream of 295/5 Orifice Plate

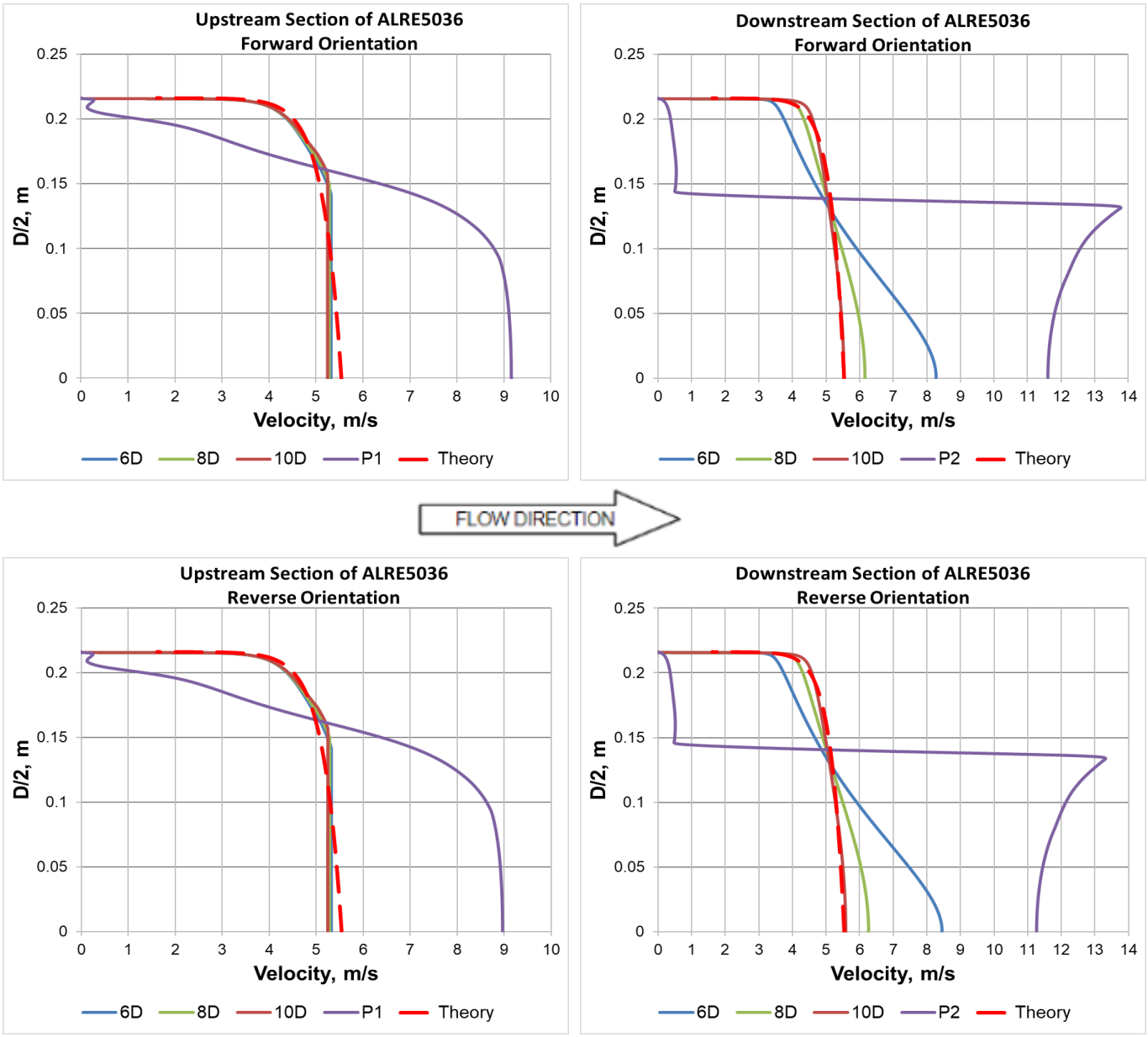

Figure 11: Velocity Profiles Upstream and Downstream of ALRE5036 Orifice Plate

Figure 12 and Figure 13 show the separation around the orifice plate edge at forward and reverse orientations.

The sharp edge of the orifice plate having a forward orientation forces the flow separate and turn abruptly. It assures that the orifice plate geometry (thickness and bevel angle) does not have a noticeable effect on the flow meter operation.

At the reverse orientation of the orifice plate geometry (thickness and bevel angle) starts having a significant effect on the flow pattern which can be compared with a nozzle. In this case the flow is turned by the 45º orifice plate bevel and remains attached to the bevel surface forming a separation bubble along.

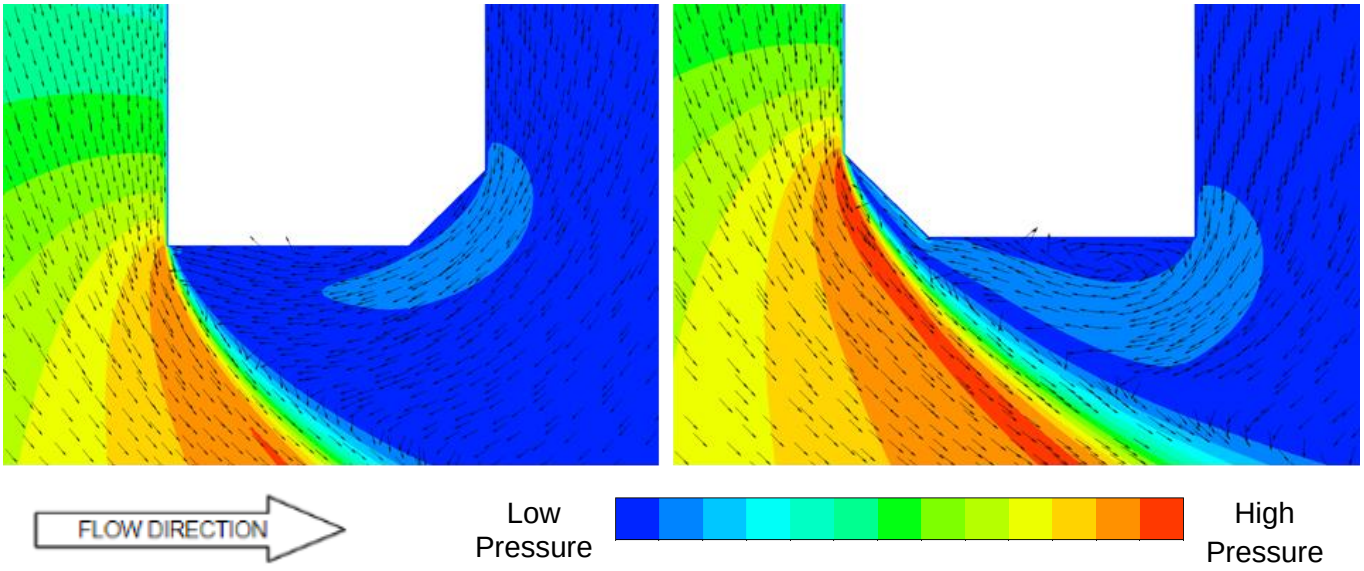

Figure 12: Separation around 295/5 Orifice Plate Edge for Forward and Reverse Orientation

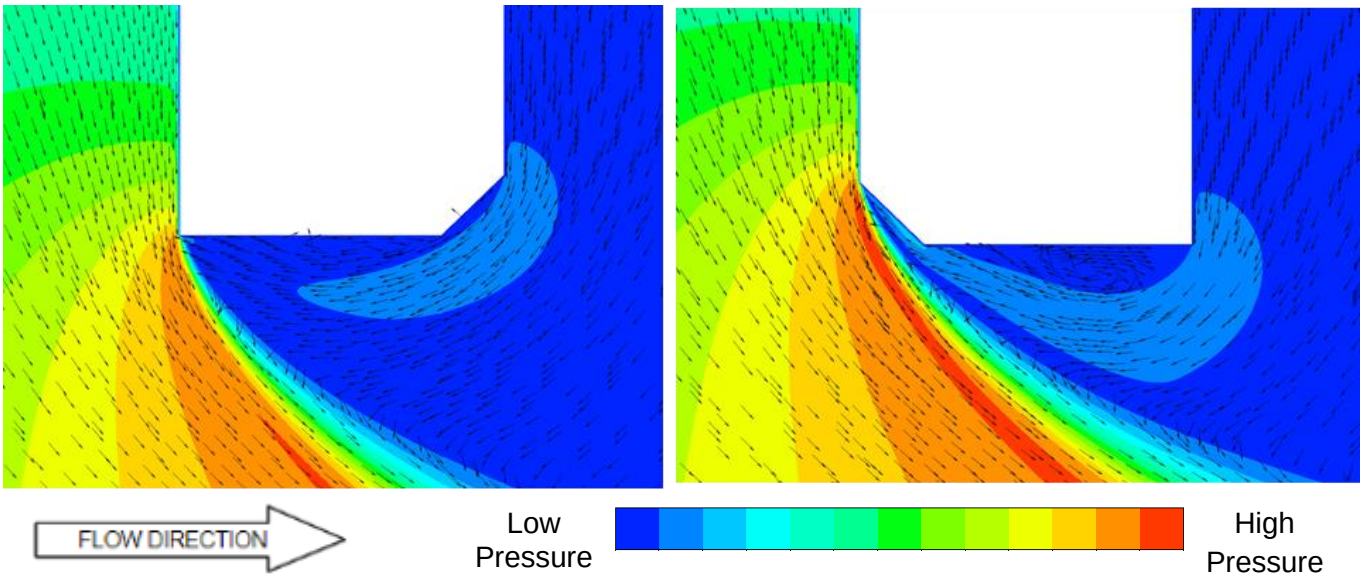

Figure 13: Separation around ALRE5036 Orifice Plate Edge for Forward and Reverse Orientation

7.2 Static Pressure and Pressure Loss

Figure 14 and Figure 15 show the pressure profile along the upstream and downstream walls of the Alrewas EM NTS offtake flow meter with the orifice plates 295/5 and ALRE5036.

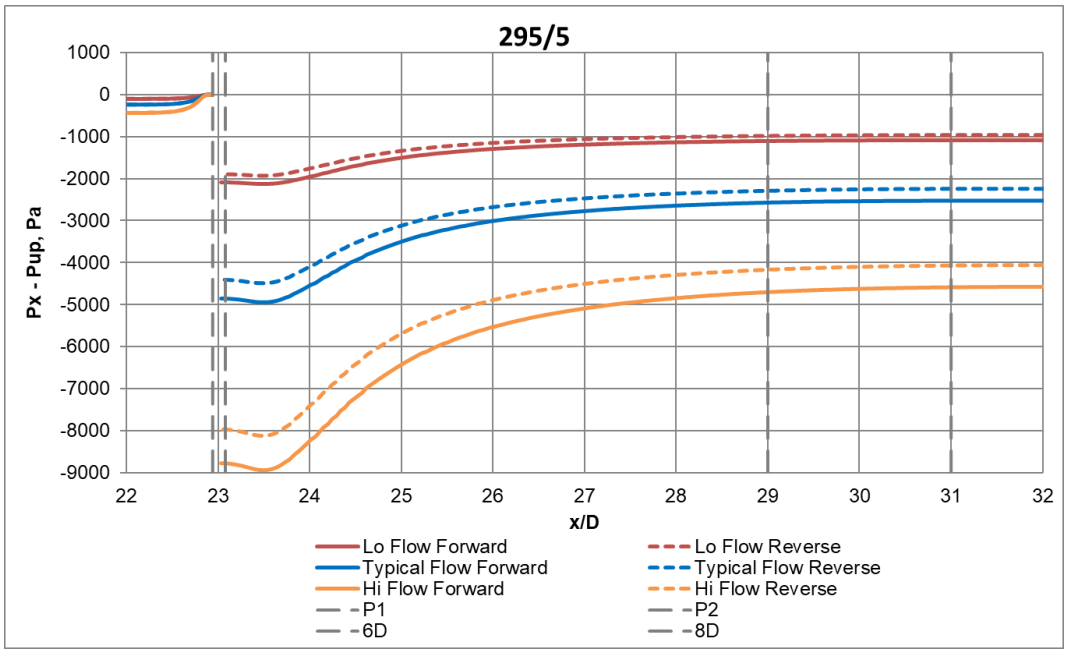

Figure 14: Static Pressure Upstream and Downstream of 295/5 Orifice Plate

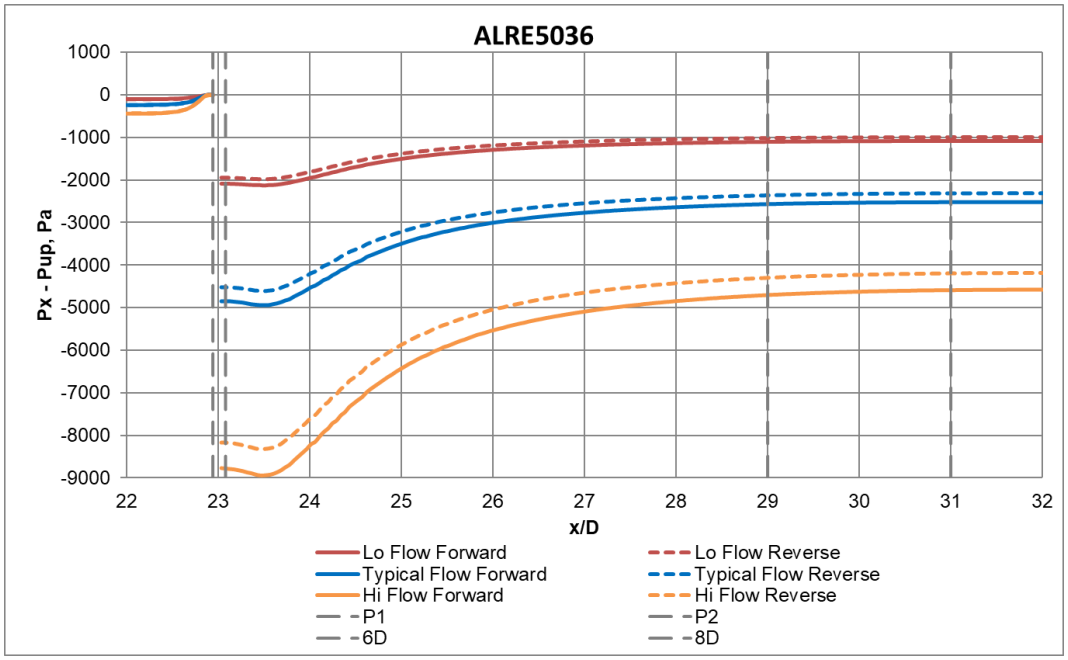

Figure 15: Static Pressure Upstream and Downstream of ALRE5036 Orifice Plate

The upstream and downstream pressure profiles are illustrated on the same graph for both forward (solid line) and reverse (broken line) orientation at three flow rates: Lo, Hi and Typical (refer to Table 8). The pressure on the wall Px is referred to the pressure Pup at upstream pressure tapping and the pressure profiles show the difference Px-Pup (Pa). The pressure tappings, 6 and 8 diameters downstream locations are indicated on the graphs by vertical broken lines.

The shape of the pressure profiles in both orientations is similar. A region of fairly constant pressure occurs just downstream of the plate where the downstream pressure tap is located, and within this region the pressure declines to its minimum, but further gradually recovers towards the exit plane.

The pressure profiles upstream and downstream are similar to the approximate profiles in ISO 5167-2 provided on Figure 16, where 1 and 2 are positions of the pressure tappings.

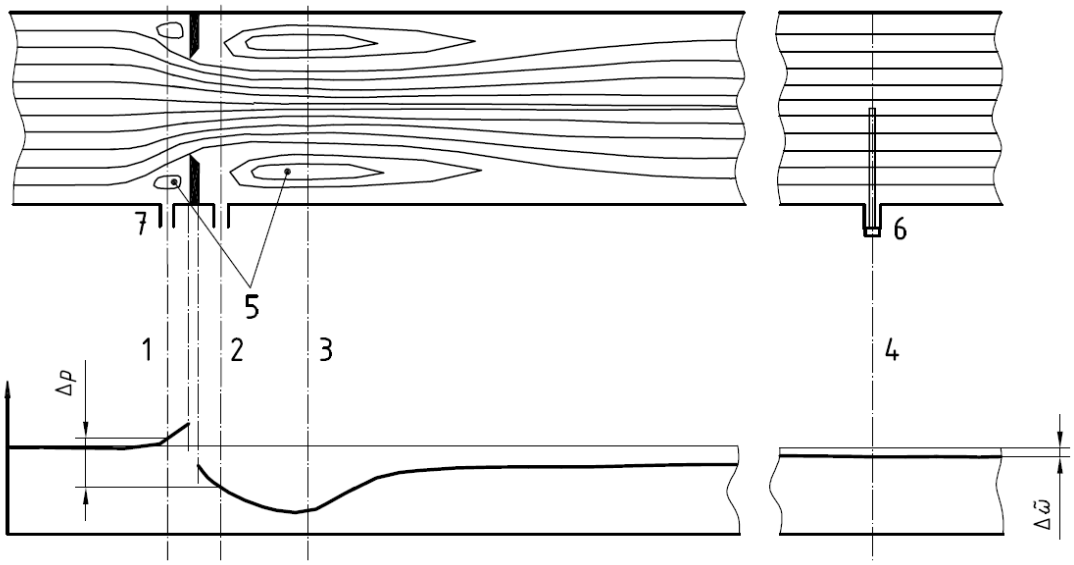

Figure 16: Approximate Profiles of Flow and Pressure in an Orifice Plate

The pressure loss is the difference in static pressure between the pressure measured at the wall of the upstream side of the orifice plate, at a section where the influence of the approach impact pressure adjacent to the plate is still negligible, and that measured on the downstream side of the plate, where the static pressure recovery by expansion of the jet may be considered as just completed (approximately 6D downstream of the orifice plate).

The pressure loss for the orifice plate, $\Delta\omega$ (Pa), is calculated as described in paragraph 5.4.1 of ISO 5167-2:2003 [6]:

$$\Delta\omega = \frac{\sqrt{1-\beta^4} - C \cdot \beta^2}{\sqrt{1-\beta^4} + C \cdot \beta^2} \cdot \Delta p \qquad \textbf{(1)}$$

Where: C is the discharge coefficient, dimensionless

β is the diameter ratio under upstream process conditions, dimensionless

Δp is the differential pressure (pressure drop), Pa

The pressure loss can be assessed using the pressure profile modelled using CFD solvers along the upstream and downstream walls of the Alrewas EM NTS offtake flow meter with the orifice plates 295/5 and ALRE5036 and shown on Figure 14 and Figure 15.

The calculated pressure loss tabulated data for three flow rates and both CFX and Fluent solvers is provided in Table 9 for 295/5 and Table 10 for ALRE5036 at 6 and 8 diameters downstream of the orifice plate for comparison.

Table 9: Comparison of CFD Computation Results for Pressure Loss of 295/5 Orifice Plate

Mass Flow Rate, kg/h (kg/s)	CFD Solver	Pressure Loss: ISO 5167-2:2003, Pa	Pressure Loss at 6D Downstream CFD, Pa	Pressure Loss Error at 6D Downstream, %	Pressure Loss at 8D Downstream CFD, Pa	Pressure Loss Error at 8D Downstream, %
86,519.10 (24.0331)	CFX	1033.00	1152.70	11.59	1105.13	6.98
	Fluent	1033.92	1102.77	6.66	1083.47	4.79
131,659.50 (36.5721)	CFX	2407.58	2600.13	8.00	2523.15	4.80
	Fluent	2405.05	2567.97	6.77	2522.63	4.89
176,799.90 (49.1111)	CFX	4347.85	4866.58	11.93	4661.58	7.22
	Fluent	4349.80	4696.99	7.98	4582.18	5.34

Table 10: Comparison of CFD Computation Results for Pressure Loss of ALRE5036 Orifice Plate

Mass Flow Rate, kg/h (kg/s)	CFD Solver	Pressure Loss: ISO 5167-2:2003, Pa	Pressure Loss at 6D Downstream CFD, Pa	Pressure Loss Error at 6D Downstream, %	Pressure Loss at 8D Downstream CFD, Pa	Pressure Loss Error at 8D Downstream, %
86,519.10 (24.0331)	CFX	1032.76	1152.53	11.60	1104.96	6.99
	Fluent	1033.67	1102.54	6.66	1083.22	4.79
131,659.50 (36.5721)	CFX	2407.02	2599.60	8.00	2522.49	4.80
	Fluent	2404.40	2567.38	6.78	2522.01	4.89
176,799.90 (49.1111)	CFX	4344.54	4717.94	8.59	4588.64	5.62
	Fluent	4348.59	4695.82	7.98	4580.98	5.34

The tabulated data is graphically presented on Figure 17. The better agreement between equation (1) and CFD computation results can be observed at 8D downstream for both orifice plates rather than at 6D as recommended in the standard.

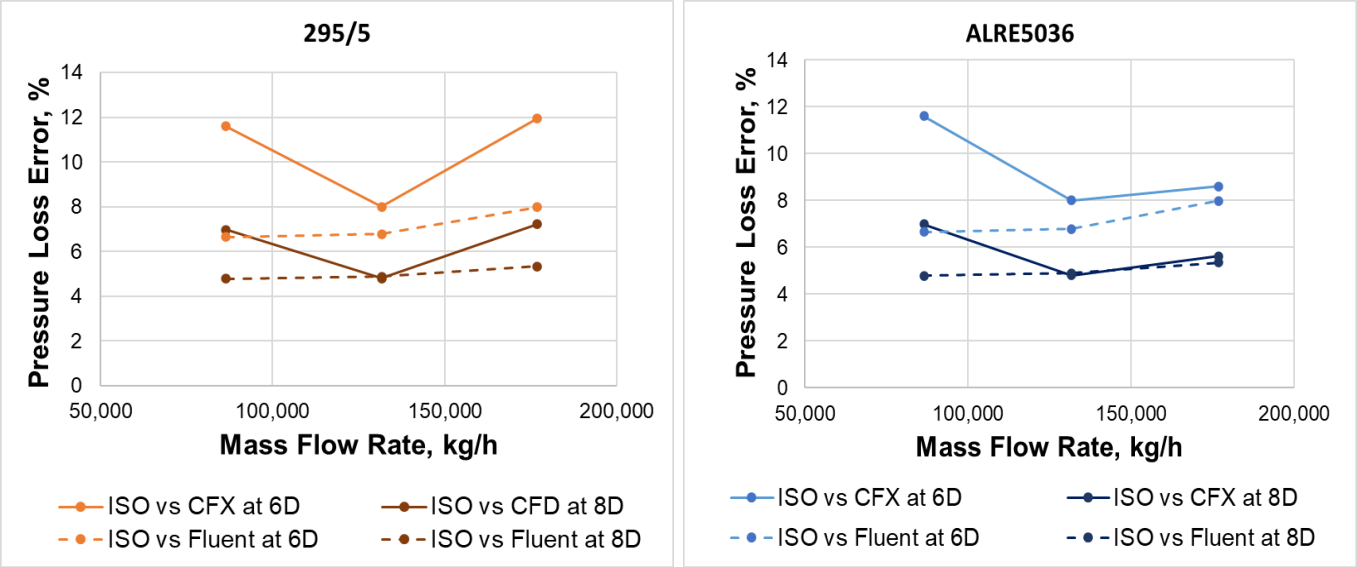

Figure 17: Comparison of ISO 5167-2:2003 and CFD Computation Results for Pressure Loss

7.3 Mass Flow Rate and Discharge Coefficient

The mass flow rate through the orifice plate is determined using the equation given in ISO 5167-2:2003 [6]:

$$q_m = \frac{C}{\sqrt{1-\beta^4}} \cdot \varepsilon \cdot \frac{\pi \cdot d^2}{4} \cdot \sqrt{2 \cdot \Delta p \cdot \rho_{us}} \quad \textbf{(2)}$$

Where:

- q_m is the mass flow rate, kg/s
- C is the discharge coefficient, dimensionless
- β is the diameter ratio under upstream process conditions, dimensionless
- d is the orifice bore diameter at upstream temperature, m
- D is the internal pipe diameter at upstream temperature, m
- ε is the expansibility factor, dimensionless
- Δp is the differential pressure (pressure drop), Pa
- ρ_{us} is the upstream process density, kg/m^3

The discharge coefficient is evaluated using the standard equation (3), where the mass flow rate is defined as a boundary condition at the inlet of the model, the pressure drop is evaluated by the CFD computation results, and other parameters are defined by the scope in section 2.4.

$$C \cdot \varepsilon = \frac{q_m \cdot \sqrt{1-\beta^4}}{\frac{\pi \cdot d^2}{4} \cdot \sqrt{2 \cdot \Delta p \cdot \rho_{us}}} \quad \textbf{(3)}$$

The results of the performed CFD computations obtained with CFX and Fluent solvers for both forward and reverse orientation of 295/5 and ALRE5036 orifice plates are tabulated in Table 11 and Table 12.

Table 11: Comparison of CFD Computation Results for Discharge Coefficient of 295/5 Orifice Plate

Mass Flow Rate, kg/h (kg/s)	CFD Solver	C·ε CFD Forward	C·ε ISO 5167-2:2003	C·ε Error CFD vs ISO 5167-2:2003, %	C·ε CFD Reverse	C·ε Correction, %
86,519.10 (24.0331)	CFX	**0.5965**	0.5978	-0.23	**0.6305**	**5.70**
	Fluent	**0.5962**	0.5978	-0.27	**0.6257**	**4.95**
131,659.50 (36.5721)	CFX	**0.5951**	0.5973	-0.37	**0.6283**	**5.58**
	Fluent	**0.5950**	0.5973	-0.38	**0.6243**	**4.92**
176,799.90 (49.1111)	CFX	**0.5939**	0.5969	-0.50	**0.6269**	**5.56**
	Fluent	**0.5942**	0.5969	-0.44	**0.6234**	**4.91**
Average Correction over the Flow Range						**5.27**

Table 12: Comparison of CFD Computation Results for Discharge Coefficient of ALRE5036 Orifice Plate

Mass Flow Rate, kg/h (kg/s)	CFD Solver	C·ε CFD Forward	C·ε ISO 5167-2:2003	C·ε Error CFD vs ISO 5167-2:2003, %	C·ε CFD Reverse	C·ε Correction, %
86,519.10 (24.0331)	CFX	**0.5965**	0.5978	-0.22	0.6213	**4.15**
	Fluent	**0.5963**	0.5978	-0.26	0.6180	**3.64**
131,659.50 (36.5721)	CFX	**0.5951**	0.5973	-0.36	0.6194	**4.07**
	Fluent	**0.5951**	0.5973	-0.37	0.6166	**3.62**
176,799.90 (49.1111)	CFX	**0.5939**	0.5969	-0.50	0.6179	**4.04**
	Fluent	**0.5943**	0.5969	-0.43	0.6158	**3.61**
Average Correction over the Flow Range						**3.85**

To assure suitability of the selected models and obtained numerical solutions the error in the discharge coefficient between the CFD computation results for the forward orientation and the ISO 2167-2:2003 calculation results is defined by equation (4) and shown on Figure 18 for both orifice plates.

$$Error = \frac{(C \cdot \varepsilon)_{CFDforward} - (C \cdot \varepsilon)_{ISO}}{(C \cdot \varepsilon)_{ISO}} \cdot 100\ \% \quad \textbf{(4)}$$

For the forward orientation the error does not exceed ±0.5 % for all modelled cases what is within the discharged coefficient uncertainty of 0.7 % stated for 0.6<β≤0.75 in the standard [6]. The error appears to be lower at lower flow rates for both CFX and Fluent solvers.

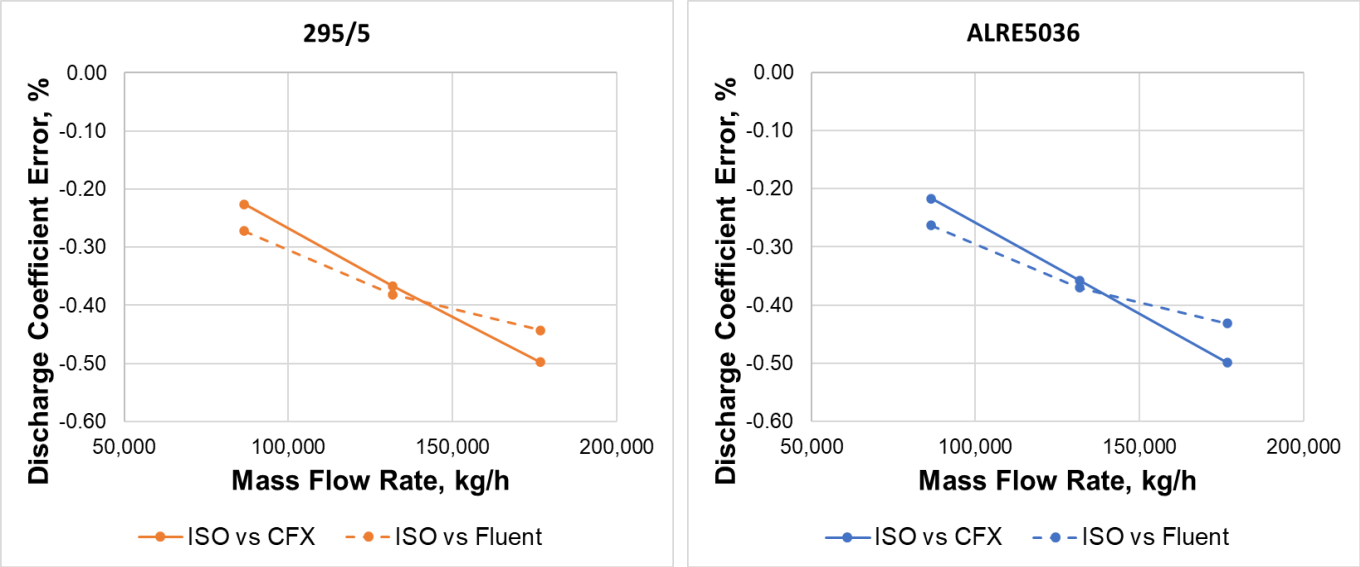

Figure 18: Comparison of ISO 5167-2:2003 and CFD Computation Results for Discharge Coefficient

The correction in the discharge coefficient between the reverse and forward orientation is calculated using equation (5) and the CFD computation results as follows:

$$Correction = \frac{(C \cdot \varepsilon)_{CFDreverse} - (C \cdot \varepsilon)_{CFDforward}}{(C \cdot \varepsilon)_{CFDforward}} \cdot 100\ \% \quad \textbf{(5)}$$

The correction is graphed as a function of flow rate on Figure 19 for both orifice plates.

It is seen from Figure 14 and Figure 15 in section 7.2 that the pressure drop in the reverse orientation is not as high as in the forward orientation. It means that in the reverse orientation **the flow rate through the orifice plate is underreported**, and **the value of the discharge coefficient is higher**.

The difference in correction slightly varies with the flow rate but can be considered as negligible as it stays well within the discharged coefficient uncertainty limit of 0.7 % calculated for $0.6<\beta\leq0.75$ using the standard [6]. In the article [11] it was concluded as well that there is no significant effect on the correction within the range of Reynolds numbers.

The discharge coefficient correction for the orifice plate 295/5 is around 5.6 % based on CFX solver and 4.9 % based on Fluent solver. The average correction is calculated as **5.27 %**.

The discharge coefficient correction for the orifice plate ALRE5036 is around 4.1 % based on CFX solver and 3.6 % based on Fluent solver. The average correction is calculated as **3.85 %**.

The difference in correction obtained by two CFD solvers for the same orifice plate is within the discharged coefficient uncertainty of 0.7 %.

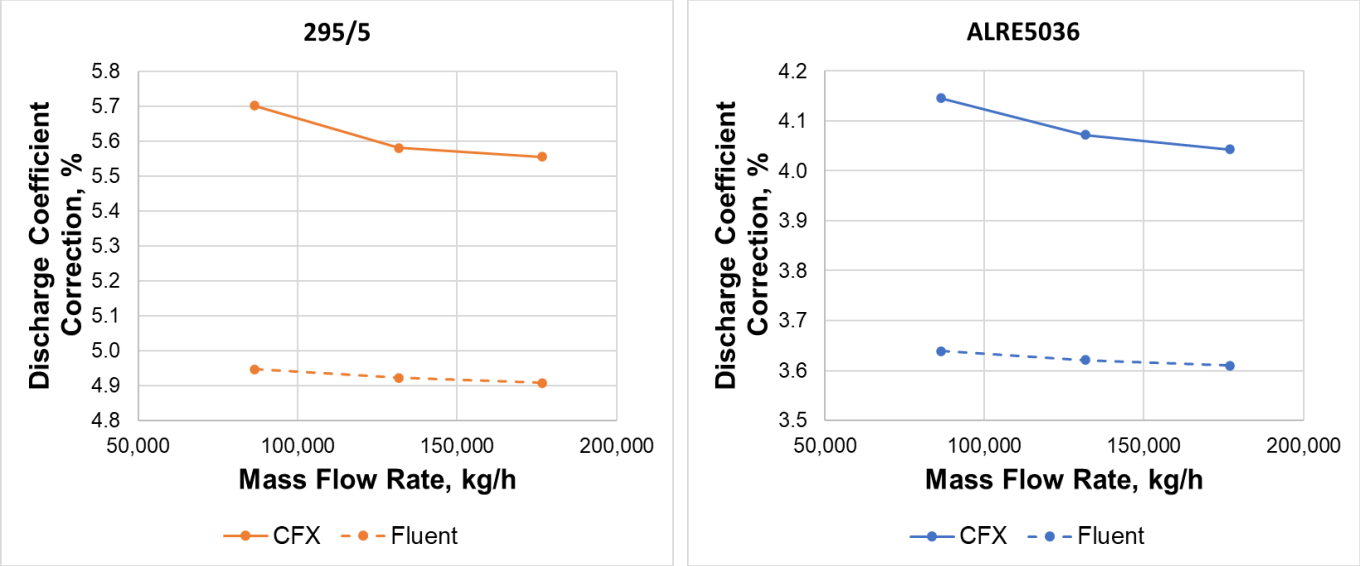

Figure 19: CFD Computation Results for Discharge Coefficient Correction

Despite similarity in geometry between the orifice plates 295/5 and ALRE5036, there is a significant difference (around 1.4 %) in the calculated correction of the discharge coefficient. Therefore, couple of examination tests have been completed aiming to check the effect of the orifice plate thickness ‘e’ and bevel angle.

In the forward orientation both solvers CFX and Fluent match very well as shown on Figure 18 as the sharp edge of the orifice plate forces the flow separate and turn abruptly. It assures that the orifice plate geometry (thickness and bevel angle) does not have a noticeable effect on the measure pressure drop across the orifice plate as shown on Figure 12, Figure 13 in section 7.1.

All changes with the reverse orientation of the orifice plate, where its geometry starts playing a significant role as the flow is turned through 45 degrees by the orifice plate bevel and remains attached to its surface forming a separation bubble along as shown on Figure 12, Figure 13 in section 7.1.

The effect of the orifice plate thickness ‘e’ and bevel angle on the correction of discharge coefficient at one flow rate is shown on Figure 20. The results were obtained only for Fluent solver and have not been compared with CFX.

With decrease of the bevel angle by 0.5º, the discharge coefficient correction drops by 0.16 % and 0.11 % for 295/5 and ALRE5036 orifice plates respectively.

With increase of the 295/5 orifice plate thickness from original of 7.015 mm to match the ALRE5036 orifice plate thickness of 7.45 mm, the discharge coefficient correction drops by **1.17 %** if the bevel angle remains the same 44.5º (the orifice plate downstream face diameter changes), and rises by 1.32 % if the bevel angle changes to 50.7º (the orifice plate downstream face diameter remains the same).

By adjusting the geometry of the orifice plate 295/5 to match the ALRE5036 orifice plate thickness and keeping the bevel angle unchanged, the calculated corrections of the discharge coefficient for 295/5 drops and matches with the correction for ALRE5036 within the bevel angle effect of 0.13 % per 0.5º described above.

Considering the results above, **the difference in correction** of the discharge coefficient for two orifice plates 295/5 and ALRE5036 **can be explained by the difference in the orifice plates thickness 'e'** of 7.015 mm and 7.45 mm respectively. The difference of 0.5º in bevel angle has significantly smaller effect.

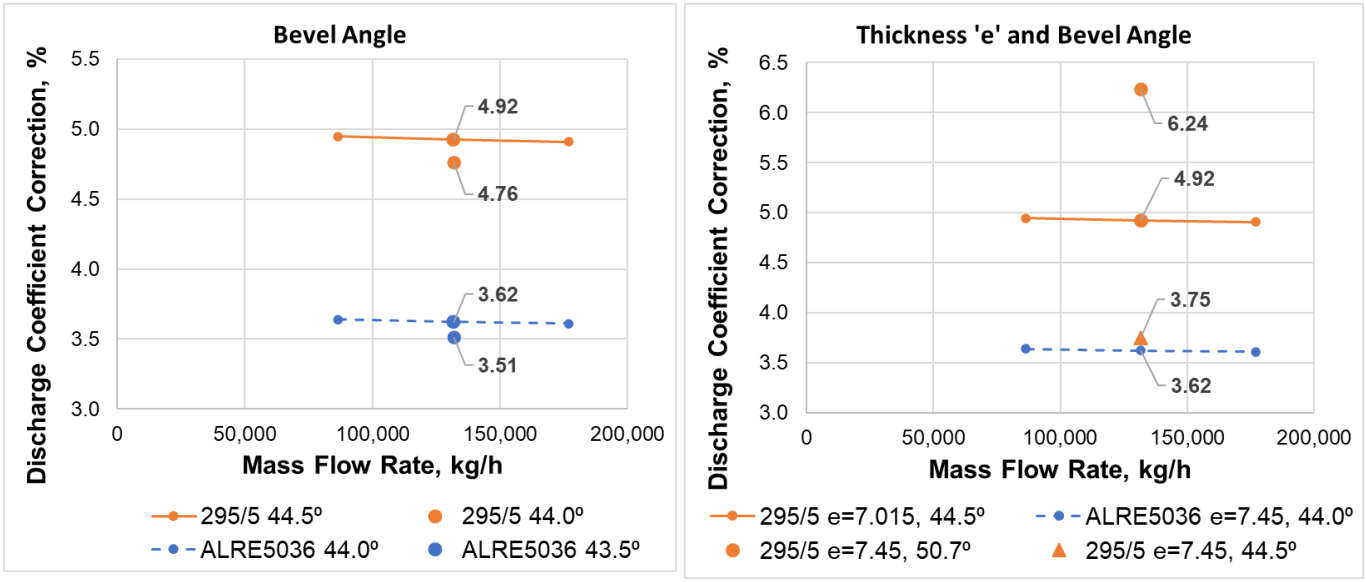

Figure 20: Effect of Orifice Plate Thickness and Bevel Angle on Discharge Coefficient Correction

The results of the examination tests allow concluding the following:

- the bigger bevel angle, the greater correction of the discharge coefficient can be expected
- the bigger the orifice plate thickness 'e' at the same bevel angle, the smaller correction of the discharge coefficient can be expected.

8 REFERENCES

[1] Alrewas EM MTD Meter Error, Executive Summary. Available in April 2022 at: https://www.gasgovernance.co.uk/sites/default/files/ggf/book/2021-03/Alrewas%20SMER%20ToR.pdf

[2] ANSYS CFX-Solver Theory Guide.

[3] ANSYS Fluent Theory Guide.

[4] ANSYS ICEM CFD Users Manual.

[5] BS 350:2004, Conversion factors for units.

[6] ISO 5167-2:2003, Measurement of fluid flow by means of pressure differential devices inserted in circular cross-section conduits running full – Part 2: Orifice plates.

[7] iVJob21088-RPT-001 V02 CFD Basis dated by 25/02/2022

[8] Menter F.R. (1994) Two-equation eddy viscosity turbulence models for engineering applications. AIAA J. 32, No 1, pp.1299–1310.

[9] Schlichting H. Boundary Layer Theory, McGraw-Hill, New York, 1968.

[10] SHIH, T-H., LIOU, W. W., SHABBIR, A., and ZHU, J. A New k-e Eddy-Viscosity Model for High Reynolds Number Turbulent Flows - Model Development and Validation. Computers Fluids, 24(3):227-238, 1995.

[11] G.J. Brown, M.J. Reader-Harris, J.J. Gibson, National Engineering Laboratory UK; and G.J. Stobie, Phillips Petroleum Co UK Ltd. Correction of readings from an orifice plate installed in reverse orientation // 18th North Sea Flow Measurement Workshop, 2000.

APPENDIX 1 ALREWAS EM DATA

Appendix 1.1 Flow Diagram of Above Ground Installation

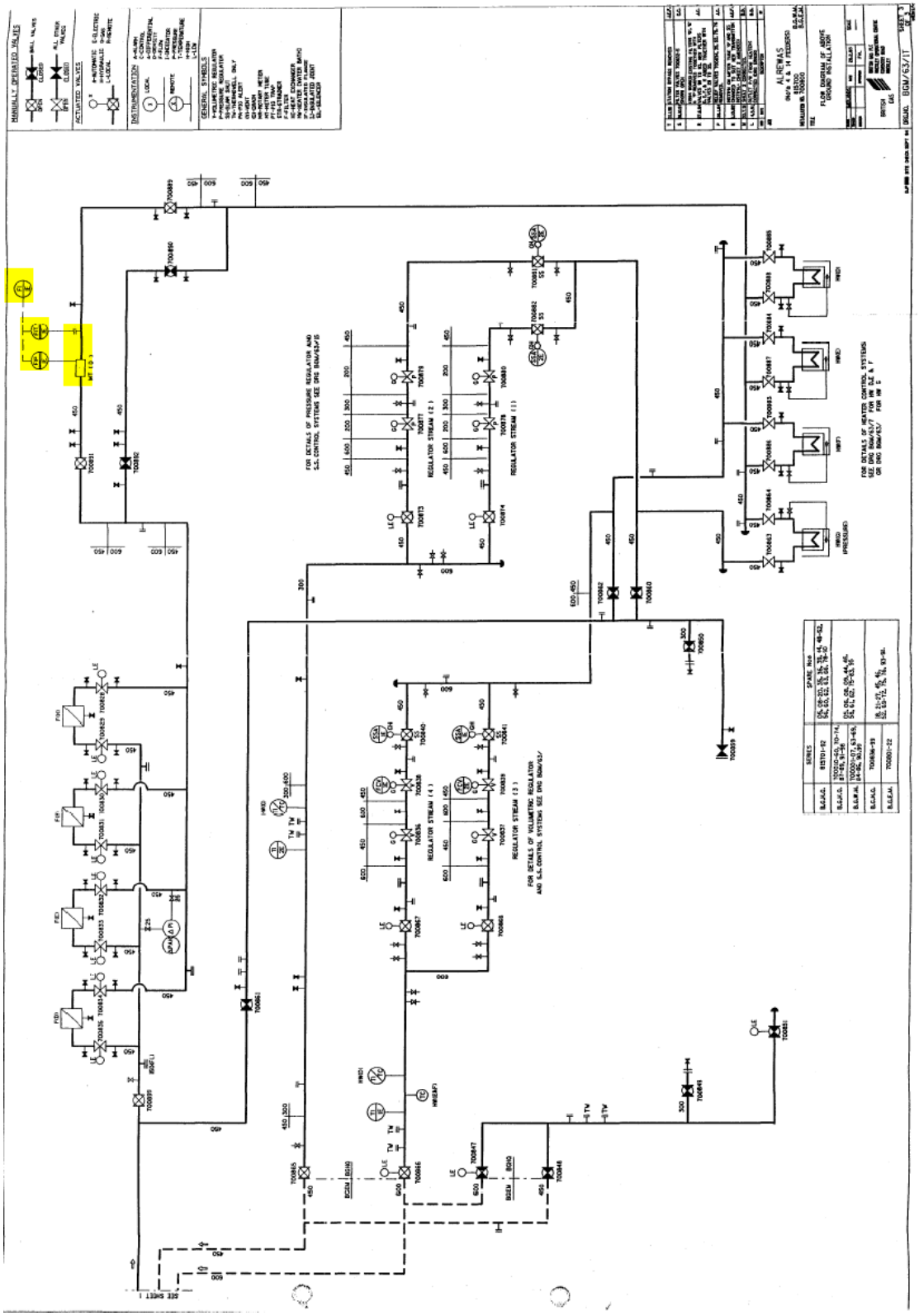

Appendix 1.2 Calibration Record of Meter Stream

RUN No. 1064 MT-D EM

ORIFICE FITTING MAKE ROBINSON
SIZE 18"
CLASS 600lb
SERIAL No. 7702835/1

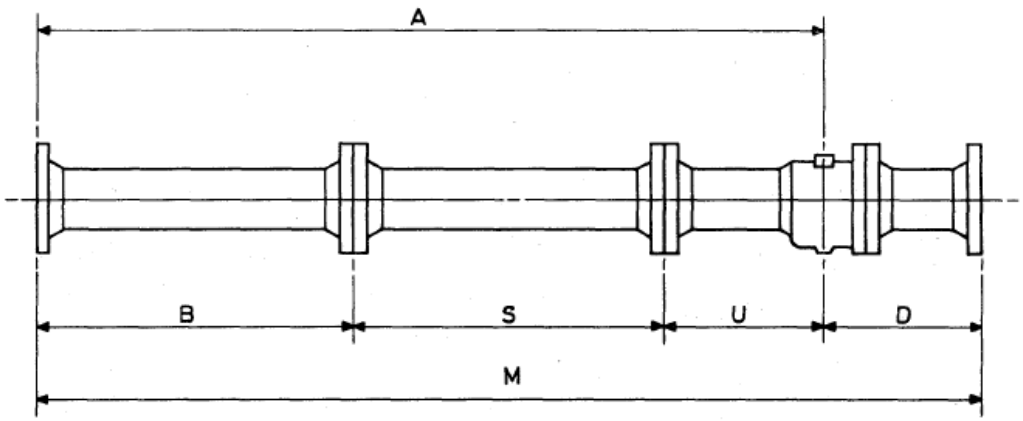

CALIBRATED SIZE IS AVERAGE OF 1 2 3		UPSTREAM SECTION				DOWNSTREAM SECTION	
		AT 1 INCH	AT 1/2 DIA.	AT 1 DIA.	AT 2 DIA.	AT 1 INCH	AT 2 DIA
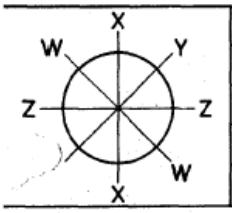	W	17.019	17.016	17.023	17.019	17.020	17.013
	X	17.021	17.019	17.024	17.019	17.019	17.016
	Y	17.013	17.013	17.034	17.014	17.018	17.019
	Z	17.015	17.013	17.057	17.013	17.019	17.023
	AV.	1:17.017	2: 17.015	3: 17.034	4: 17.016	1: 17.019	2: 17.018
NOM. I.D. =		CALIBRATED SIZE		17.022		17.018	

	DIMENSION	ACTUAL DIM.		DIMENSION	ACTUAL DIM.
A			M	43' 6-1/16"	43' 6 1/16"
B			E		
S			P		
U	33' 0 1/8"	33' 0 1/8"	Q		
D	10' 5 7/8"	10' 5 7/8"	R		

HYDROSTATIC TEST : 1 hr. min. HRS. AT 2175 P. S. I. KCF / CH^2

HEECO INTERNATIONAL LTD.
THETFORD, NORFOLK
PHONE 4761 (STD. 0842)

MATERIAL | SCALE | DRN. | DATE

TITLE
METER RUN
CALIBRATION RECORD

APPENDIX 2 CFX AND FLUENT SOLVER SETTINGS

Appendix 2.1 CFX Settings

Appendix 2.1.1 Material Properties

Tab	Setting	Value
Basic Setting	Option	Pure Substance
	Material Group	Calorically Perfect Ideal Gases
	Thermodynamic State	Gas
Material Properties	Option	General Material
	Equation of State-> Ideal Gas->Molar Mass (Note - gas compressibility is considered)	20.674021 [kg/kmol]
	Transport Properties ->Dynamic Viscosity	1.204e-5 [Pa*s]

Appendix 2.1.2 Domain Settings

Tab	Setting	Value
Basic Settings	Domain Type	Fluid Domain
	Boundary Details Pressure->Reference Pressure	(56+1.01325) [bar]
	Buoyancy Model->Option	Non Buoyant
	Heat Transfer-> Option	Isothermal
	Heat Transfer-> Fluid Temperature	8.5 [C]
	Turbulence -> Option	SST
	Turbulence -> Wall Function	Automatic

Appendix 2.1.3 Expressions Connecting Modelling Parameters

Name	Definition
MFR	Case 01: 86519.1 [kg/hr] Case 02: 131659.5 [kg/hr] Case 03: 176799.9 [kg/hr]
MFRInlet	MFR *0.000407705 [m^2] / S0
S0	d0 * d0 * pi / 4
d0	432.3053 [mm]

Appendix 2.1.4 Boundary Conditions

Boundary Inlet

Tab	Setting	Value
Basic Settings	Boundary Type	Inlet
Boundary Details	Flow regime	Subsonic
	Mass and Momentum -> Mass Flow Rate	MFR
	Turbulence	Medium (Intensity 5%)
	Flow Direction->Option	Normal to Boundary Condition

Boundary Outlet

Tab	Setting	Value
Basic Settings	Boundary Type	Opening
Boundary Details	Flow regime	Subsonic
	Mass and Momentum -> Opening Pres. and Dirn	0
	Flow Direction->Option	Normal to Boundary Condition
	Turbulence	Medium (Intensity 5%)

Boundary Wall

Tab	Setting	Value
Basic Settings	Boundary Type	Wall
Boundary Details	Mass and Momentum	No Slip Wall
	Wall Roughness	Smooth Wall

Boundary Sym

Tab	Setting	Value
Basic Settings	Boundary Type	Symmetry

Appendix 2.2 Fluent Settings

Appendix 2.2.1 Material Property

Tab	Setting	Value
Material Properties	Option	General Material
	Density	Ideal Gas
	Cp	Piecewise-polynomial
	Thermal Conductivity	0.0332 [w/m-k]
	Viscosity	1.204e-5 [kg/m-s]
	Molecular Weight (Note - gas compressibility is considered)	20.67402 [kg/kmol]

Appendix 2.2.2 Domain Setting

Tab	Setting	Value
Operating Conditions	Operating Pressure	5701325 Pa
	Reference Pressure Location X	0 m
	Reference Pressure Location Y	0 m

Appendix 2.2.3 Model Settings

Tab	Setting
Energy	On
Viscous Model	K-omega SST

Appendix 2.2.4 Boundary Conditions

Boundary Inlet

Tab	Setting	Value
Basic Settings	Boundary Type	Mass-flow-inlet
Boundary Details	Direction Specification Method	Normal to Boundary
	Mass flow rate	24.03308333 [kg/s] 36.57208333 [kg/s] 49.11108333 [kg/s]
	Initial gauge pressure	0 [Pa]
	Turbulence	Intensity 5%
	Total temperature	8.5 [C]

Boundary Outlet

Tab	**Setting**	**Value**
Basic Settings	Boundary Type	Pressure-outlet
Boundary Details	Gauge Pressure	0 [Pa]
	Backflow Total temperature	8.5 [C]

Boundary Wall

Tab	**Setting**	**Value**
Basic Settings	Boundary Type	Wall
Boundary Details	Shear Condition	No Slip
Boundary Details	Wall Roughness	Standard
	Roughness Height	0 [m]

Boundary Axe

Tab	**Setting**	**Value**
Basic Settings	Boundary Type	Axis

APPENDIX 3 MODEL COMPARISON

This section provides the comparison of the CFD computation results obtained using the model setup proposed in the present report with the modelling data published in the article covering the corrections from the orifice plate installed in reverse orientation on the Judy platform [11].

The model geometry, grid, setup and boundary conditions are compared in Table 13. The plate and pipe dimensions, and process conditions are as detailed in the article [11].

Table 13: Differences in Model Setup for Judy Orifice Plate

Parameter	Article [11]	Present Report
CDF package	Fluent	CFX, Fluent
Turbulence Model	realisable k-ε [10]	k-ω SST [8]
Number of elements	130,000	500,000
Mesh Grid	1.05 mm size of elements 8 elements along the orifice-edge 14 elements along the bevel.	0.1 mm size of elements 22 elements along the orifice-edge 70 elements along the bevel.
Upstream and Downstream Length	3D	23D
Inlet Boundary Conditions	Fully developed flow	Mass flow rate and evenly distributed velocity across the pipe

The comparison of the CFD computation results obtained from the article [11] and by using the model setup proposed in the present report is provided in the sections below.

Appendix 3.1 Separation around Edge of Judy Orifice Plate

Figure 21 and Figure 22 show the separation around the orifice plate edge at forward and reverse orientations of Judy Orifice Plate and show a reasonable qualitative agreement.

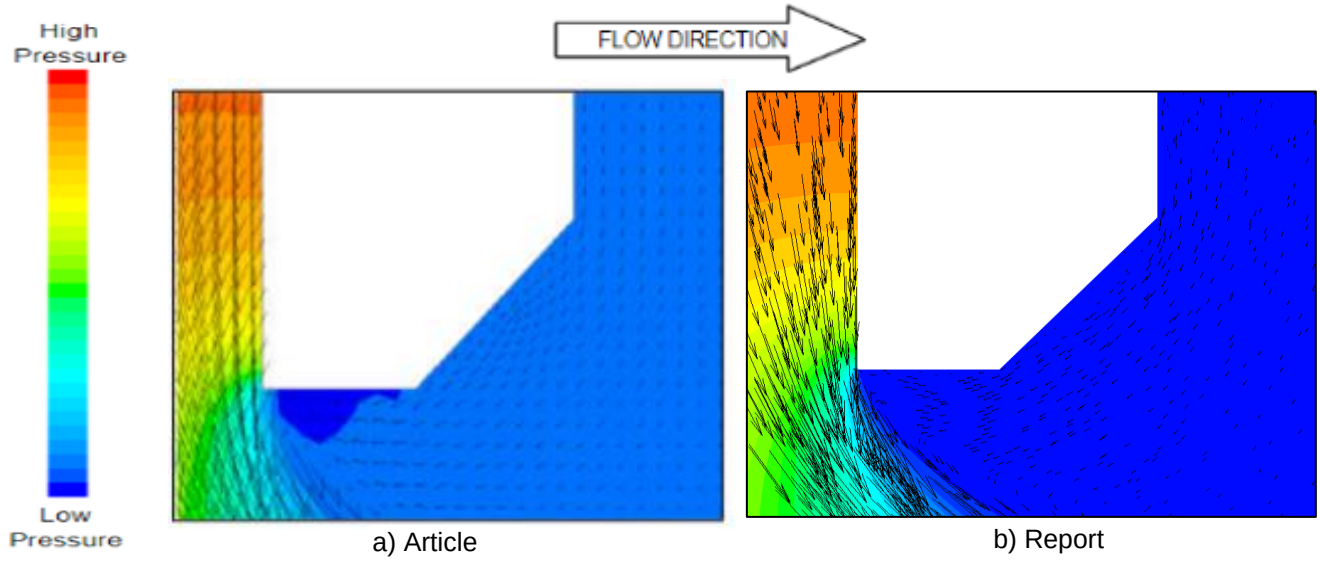

Figure 21: Separation around Edge for Forward Direction of Judy Orifice Plate

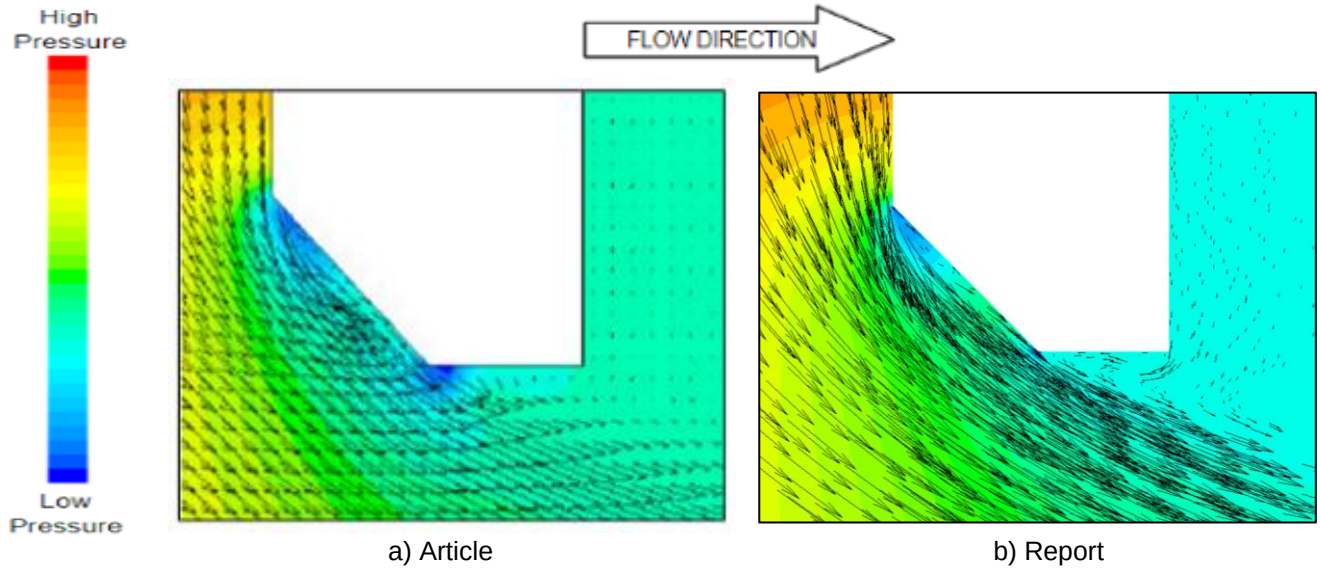

Figure 22: Separation around Edge for Reverse Direction of Judy Orifice Plate

Appendix 3.2 Static Pressure of Judy Orifice Plate

Figure 23 shows the comparison of the pressure variation along the upstream and downstream walls of the Judy orifice plate (a) obtained from the article and modelled using Fluent Solver (b) with the settings provided in section 6.

The pressure variation curves are comparable and have similar shape and magnitude. The pressure drops of approximately 21,000 Pa for the plate in the forward direction, and of approximately 15,000 Pa for the plate in the reverse direction are obtained.

ISO 5167-2:2003 [6] quotes uncertainty in discharge coefficient as ±0.5 % (for 0.2≤*β*≤0.6) and the corresponding uncertainty in pressure drop would be ±1.0 % as indicated by error bars on Figure 23 (b). On Figure 23 (a) the error bars correspond to ±1.2 % uncertainty in pressure drop or ±0.6 % in discharge coefficient as the earlier version of the standard ISO 5167-1:1991 was used.

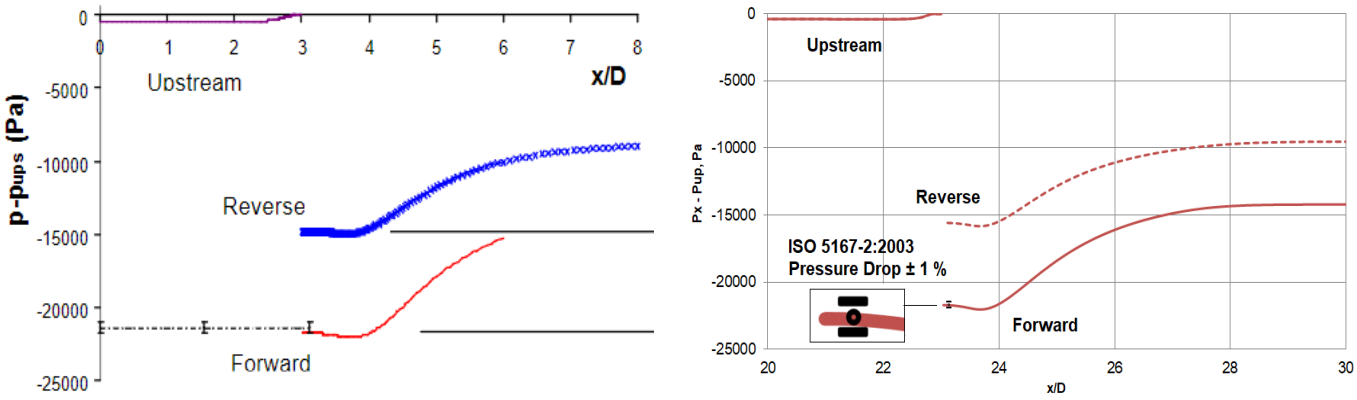

a) Article b) Report

Figure 23: Comparison of Static Pressure Upstream and Downstream of Judy Orifice Plate

Appendix 3.3 Change in Discharge Coefficient of Judy Orifice Plate

Table 11 and Figure 24 show the results of the performed computations obtained with CFX and Fluent solvers in comparison with one of the cases provided in article [11].

For the forward orientation the best match with ISO 5167-2:2003 is observed for the CFX computation result with the error of minus 0.43 % that is within the discharged coefficient uncertainty of 0.5 % stated for 0.2≤β≤0.6 in the standard [6].

Table 14: Comparison of CFD Computation Results for Judy Orifice Plate

Source	Re_D	β=d/D	e	b	b/d	b/E	ε·C ISO 5167-2:1991	ε·C ISO 5167-2:2003	ε·C CFD Forward	Error CFD vs ISO 5167-2:2003, %	ε·C CFD Reverse	ε·C Correction, %
Article	$12.08 \cdot 10^6$	0.5802	4.5	5.02	0.033	0.53	0.6041*	**0.6028**	0.5990	**-0.64**	0.7289	21.67
CFD Fluent Solution							0.6038		0.5995	**-0.55**	0.7064	17.83
CFD CFX Solution									0.6002	**-0.43**	0.7009	16.77

* expansibility **ε** is not considered

Data from offshore verification trials showed the correction (increase) in discharge coefficient of approximately 19.4 %, and 70 % of corrections calculated on a point-by-point basis for 108 points lie between 15 and 25 %.

The Fluent computation result lies closer to the offshore verification trials with correction of 17.83 % as detailed in Table 12 and shown on Figure 24, where the CFX and Fluent computation results are indicated by an alternative to black colour.

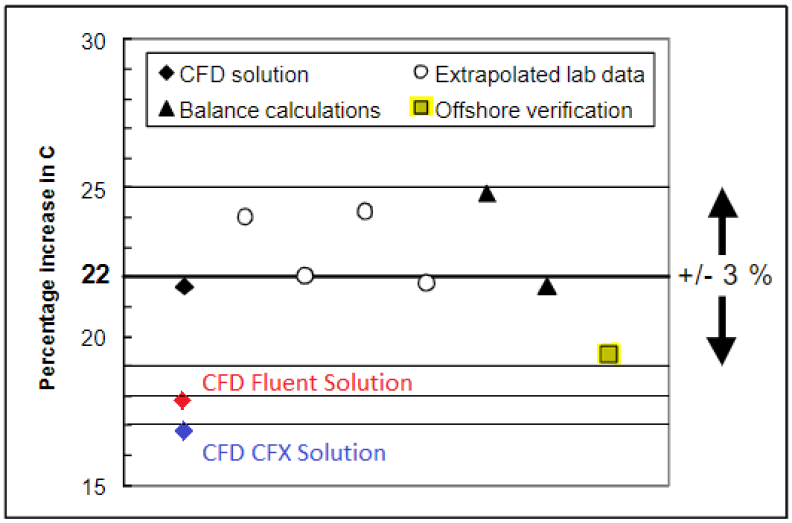

Figure 24: Summary of Results of Judy Orifice Plate

Table 15: Comparison of CFD Computations with Offshore Verification for Judy Orifice Plate

Source	ε·C CFD Forward	ε·C CFD Reverse	ε·C Correction: CFD Computations, %	ε·C Correction: Offshore Verification	Difference, %
Article	0.5990	0.7289	21.67	19.4	**11.70**
CFD Fluent Solution	0.5995	0.7064	17.83		**-8.12**
CFD CFX Solution	0.6002	0.7009	16.77		**-13.57**